

QIR_2004.pdf

by Pranowo Pranowo

Submission date: 08-Aug-2019 09:17AM (UTC+0700)

Submission ID: 1158485610

File name: Adaptive_Multiresolution_Scheme_Based_on_Haar_Wavelets.doc (1.82M)

Word count: 1593

Character count: 9035

Adaptive Multiresolution Scheme Based on Haar Wavelets For Acoustic Wave Propagation

¹⁰ Pranowo¹ & F. Soesianto²

¹Teknik Informatika Universitas Atma Jaya Yogyakarta
Jl. Babarsari 43 Yogyakarta 55281 Indonesia
E-mail: pran@mail.uajy.ac.id

²Teknik Elektro Universitas Gadjah Mada
Jl. Grafika 2 Yogyakarta 55281 Indonesia

Abstract

In this paper, we present the multiresolution time-domain method (MRTD) based on Haar wavelets for acoustic wave propagation. The numerical method has the ability to represent functions at different levels of resolution. Wavelets are localized in space, which means that the solution can be refined in regions of high pressure gradient without having to regenerate the mesh for the entire domain. We employ a mesh adaption in physical space dynamically using wavelet thresholding to follow the propagation of the wave. Using grid adaption, the computational effort can be reduced. Computed acoustic fields are compared to the exact solution, the comparison shows a good agreement.

Key words: adaptive, multiresolution time-domain, Haar wavelet, acoustic fields.

I. Introduction

Recently wavelet theory has been a field intensive research for mathematicians and engineers. The properties of wavelet such as time/space and frequency localization encouraged many researchers to study wavelet for solving partial differential equations (Chiavassa, 1997). Wavelet based techniques have shown significant promise in area of numerical modeling of physical phenomena that contain high gradient or sharp transition (Sarris et. al., 2000). Examples of the later are formation of shock waves, electromagnetic and acoustic wave propagation. The modelling of engineering system involving acoustic wave interactions was dominated by frequency-domain methods. The frequency-domain methods can not be applied for nonlinear problems and broadband linear excitations.

For those reasons, time-domain methods have greater potential for solving complex problems than frequency-domain methods. Time-domain methods directly simulate the physical systems by making discrete approximation for the time and spatial derivatives to turn the partial differential equations into a system of algebraic equations. Yee introduced the first time-domain method in 1996 (Nguyen, 1996). This method computes electric and magnetic fields that are staggered in space and time and can be interpreted as standard leapfrog method and well known as Yee's scheme FDTD. Based on Yee's scheme, Botteldoreen developed finite difference time domain for solving room acoustic problems (1995). Schneider et al. used FDTD for solving scattered acoustic waves (1998).

Some new schemes have also started with Yee's scheme but were extended for greater accuracy rather than for geometry. Nguyen (1996) used upwind leapfrog method for solving acoustics and electromagnetics. Kim (1997) developed upwind leapfrog for solving acoustic and aeroacoustic wave propagation problems. More recently work on multiresolution time-domain techniques have been published by Katehi's group from University of Michigan (Sarris, 2001; Tentzeris, 1997). They developed multiresolution time-domain (MRTD) method to analyze electromagnetic fields. In the MRTD scheme, the field components are expanded by using scaling and wavelet function then tested with using scaling and wavelet function through Galerkin's procedure. In this paper, Haar scaling and wavelet function are used to represent pressure and velocity fields. Based on Dogaru's (1999) work, we extended MRTD method for solving acoustic equations.

II. Formulations

A. One-dimensional Formulation

The application of the MRTD method to the simple case of one-dimensional system of non-dimensionalized acoustic equations is considered.

$$\frac{\partial u}{\partial t} = -\frac{\partial p}{\partial x} \quad (1a)$$

$$\frac{\partial p}{\partial t} = -\frac{\partial u}{\partial x} \quad (1b)$$

1 The spatial variation of pressure and velocity fields is defined by a basis composed of scaling and wavelet functions. The Haar scaling functions are defined as orthogonal translations:

$$\phi_k(x) = \phi\left(\frac{x}{\Delta x} - k\right) \quad (2)$$

of $\phi(x) = \chi_{[0,1)}(x)$, with $\chi_{[a,b)}(x) = 1$, when $x \in [a,b)$ and zero otherwise. In this notation Δx is the cell size in x-direction. Haar wavelet function is defined as:

$$\psi_k(x) = \psi\left(\frac{x}{\Delta x} - k\right) \quad (3)$$

The function $\psi(x) = \chi_{[0,1/2)}(x) - \chi_{[1/2,1)}(x)$, whose dilations and translations yield the wavelet basis, is the well-known Haar mother wavelet function.

The temporal variation of fields is described in terms of pulse functions

$$h_k(t) = h\left(\frac{t}{\Delta t} - k\right) \quad (4)$$

with $h(t) = \chi_{[0,1)}(t)$ and Δt being the time step.

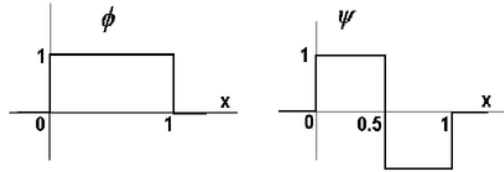
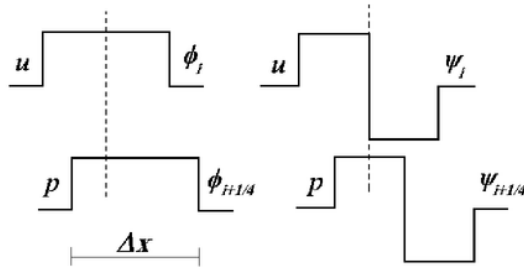


Fig. 1. Scaling and wavelet function

We consider the expansion of velocity and pressure fields using scaling functions and one level wavelet functions:

$$u = \sum_{i=0}^I \sum_{n=0}^N h_n(t) (u_{i,n}^\phi \phi_i(x) + u_{i,n}^\psi \psi_i(x)) \quad (5a)$$

$$p = \sum_{i=0}^I \sum_{n=0}^N h_{n+1/2}(t) (p_{i+1/4,n+1/2}^\phi \phi_{i+1/4}(x) + p_{i+1/4,n+1/2}^\psi \psi_{i+1/4}(x)) \quad (5b)$$



5 Fig.2. Support of the basis functions in the velocity and pressure expansions using one level of Haar wavelets

Figure 2 indicates that the support of the scaling/wavelet functions corresponding to velocity and pressure fields are displaced by one quarter of a cell. Now sample equation (1.a) according Galerkin's procedure, using $h_{n+1/2}(\phi_i(x) + \psi_i(x))$ as testing function.

$$\int_{-\infty}^{\infty} \int_{-\infty}^{\infty} \left(\frac{\partial u}{\partial t} + \frac{\partial p}{\partial x} \right) h_{n+1/2}(t) \phi_i(x) dx dt = 0$$

$$= (u_{i,n+1}^{\phi} - u_{i,n}^{\phi}) \Delta x + \left((p_{i+1/4,n+1/2}^{\phi} - p_{i-3/4,n+1/2}^{\phi}) + (-p_{i+1/4,n+1/2}^{\psi} + p_{i-3/4,n+1/2}^{\psi}) \right) \Delta t$$
(6a)

$$\int_{-\infty}^{\infty} \int_{-\infty}^{\infty} \left(\frac{\partial u}{\partial t} + \frac{\partial p}{\partial x} \right) h_{n+1/2}(t) \psi_i(x) dx dt = 0$$

$$= (u_{i,n+1}^{\psi} - u_{i,n}^{\psi}) \Delta x + \left((p_{i+1/4,n+1/2}^{\phi} - p_{i-3/4,n+1/2}^{\phi}) + (3p_{i+1/4,n+1/2}^{\psi} + p_{i-3/4,n+1/2}^{\psi}) \right) \Delta t$$
(6b)

The sampling process continues by testing equation (1.b) with $h_n(\phi_{i+1/4}(x) + \psi_{i+1/4}(x))$. After re-arranging the terms, the final expressions for the MRTD equations are:

$$u_{i,n+1}^{\phi} = u_{i,n}^{\phi} + \frac{\Delta t}{\Delta x} (p_{i+1/4,n+1/2}^{\phi} - p_{i-3/4,n+1/2}^{\phi} - p_{i+1/4,n+1/2}^{\psi} + p_{i-3/4,n+1/2}^{\psi})$$
(7a)

$$u_{i,n+1}^{\psi} = u_{i,n}^{\psi} + \frac{\Delta t}{\Delta x} (p_{i+1/4,n+1/2}^{\phi} - p_{i-3/4,n+1/2}^{\phi} + 3p_{i+1/4,n+1/2}^{\psi} + p_{i-3/4,n+1/2}^{\psi})$$
(7b)

$$p_{i+1/4,n+1/2}^{\phi} = p_{i+1/4,n-1/2}^{\phi} + \frac{\Delta t}{\Delta x} (u_{i+1,n}^{\phi} - u_{i,n}^{\phi} + u_{i+1,n}^{\psi} - u_{i,n}^{\psi})$$
(7c)

$$p_{i+1/4,n+1/2}^{\psi} = p_{i+1/4,n-1/2}^{\psi} + \frac{\Delta t}{\Delta x} (-u_{i+1,n}^{\phi} + u_{i,n}^{\phi} - u_{i+1,n}^{\psi} - 3u_{i,n}^{\psi})$$
(7d)

B. Extension to Two-Dimensions

The combination of a Haar scaling function and one wavelet level, in two-dimensions, is shown in fig.3. The acoustic wave propagation is governed by the following equations:

$$\frac{\partial u}{\partial t} = -\frac{\partial p}{\partial x}$$
(8a)

$$\frac{\partial v}{\partial t} = -\frac{\partial p}{\partial y}$$
(8b)

$$\frac{\partial p}{\partial t} = -\left(\frac{\partial u}{\partial x} + \frac{\partial v}{\partial y} \right)$$
(8c)

As an example, we discretize the equation (8c). The pressure field can be expanded using scaling and one level wavelet as

$$p = \sum_{i=0}^I \sum_{j=0}^J \sum_{n=0}^N h_{n+1/2}(t) \begin{bmatrix} p_{i+1/4,j+1/4}^{\phi} \phi_{i+1/4}(x) \phi_{j+1/4}(y) + \\ p_{i+1/4,j+1/4}^{\psi} \psi_{i+1/4}(x) \psi_{j+1/4}(y) + \\ p_{i+1/4,j+1/4}^{\psi\phi} \psi_{i+1/4}(x) \phi_{j+1/4}(y) + \\ p_{i+1/4,j+1/4}^{\phi\psi} \phi_{i+1/4}(x) \psi_{j+1/4}(y) \end{bmatrix}$$
(9)

With similar expressions for velocity fields. The testing functions for equation (8c) are:

$$h_n(t) \left(\phi_{i+1/4}(x) \phi_{j+1/4}(y) + \phi_{i+1/4}(x) \psi_{j+1/4}(y) + \right.$$

$$\left. \psi_{i+1/4}(x) \phi_{j+1/4}(y) + \psi_{i+1/4}(x) \psi_{j+1/4}(y) \right)$$
(10)

The usual discretization procedure yields the following set of equations (only p update equations are given here):

$$p_{i+1/4,j+1/4,n+1/2}^{\phi\phi} = p_{i+1/4,j+1/4,n-1/2}^{\phi\phi} - \frac{\Delta t}{\Delta x} (u_{i+1,j+1/4,n}^{\phi\phi} - u_{i,j+1/4,n}^{\phi\phi} + u_{i+1,j+1/4,n}^{\psi\psi} - u_{i,j+1/4,n}^{\psi\psi}) - \frac{\Delta t}{\Delta y} (v_{i+1/4,j+1,n}^{\phi\phi} - v_{i+1/4,j,n}^{\phi\phi} + v_{i+1/4,j+1,n}^{\psi\psi} - v_{i+1/4,j,n}^{\psi\psi}) \quad (10a)$$

$$p_{i+1/4,j+1/4,n+1/2}^{\phi\psi} = p_{i+1/4,j+1/4,n-1/2}^{\phi\psi} - \frac{\Delta t}{\Delta x} (u_{i+1,j+1/4,n}^{\phi\psi} - u_{i,j+1/4,n}^{\phi\psi} + u_{i+1,j+1/4,n}^{\psi\psi} - u_{i,j+1/4,n}^{\psi\psi}) + \frac{\Delta t}{\Delta y} (-v_{i+1/4,j+1,n}^{\phi\phi} + v_{i+1/4,j,n}^{\phi\phi} - v_{i+1/4,j+1,n}^{\psi\psi} + 3v_{i+1/4,j,n}^{\psi\psi}) \quad (10b)$$

$$p_{i+1/4,j+1/4,n+1/2}^{\psi\phi} = p_{i+1/4,j+1/4,n-1/2}^{\psi\phi} - \frac{\Delta t}{\Delta x} (-u_{i+1,j+1/4,n}^{\phi\phi} + u_{i,j+1/4,n}^{\phi\phi} - u_{i+1,j+1/4,n}^{\psi\psi} + 3u_{i,j+1/4,n}^{\psi\psi}) + \frac{\Delta t}{\Delta y} (v_{i+1/4,j+1,n}^{\psi\phi} - v_{i+1/4,j,n}^{\psi\phi} + v_{i+1/4,j+1,n}^{\psi\psi} - v_{i+1/4,j,n}^{\psi\psi}) \quad (10c)$$

$$p_{i+1/4,j+1/4,n+1/2}^{\psi\psi} = p_{i+1/4,j+1/4,n-1/2}^{\psi\psi} - \frac{\Delta t}{\Delta x} (-u_{i+1,j+1/4,n}^{\phi\psi} + u_{i,j+1/4,n}^{\phi\psi} - u_{i+1,j+1/4,n}^{\psi\psi} + 3u_{i,j+1/4,n}^{\psi\psi}) + \frac{\Delta t}{\Delta y} (-v_{i+1/4,j+1,n}^{\psi\phi} + v_{i+1/4,j,n}^{\psi\phi} - v_{i+1/4,j+1,n}^{\psi\psi} + 3v_{i+1/4,j,n}^{\psi\psi}) \quad (10d)$$

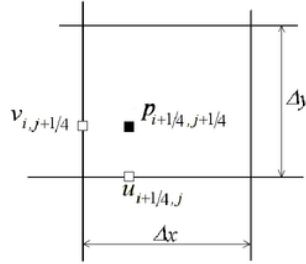


Fig. 4. Velocity and pressure components displacement

C. Wall Boundary Conditions

The boundary was assumed to be perfect electric conductor (PEC). MRTD scheme would model the PEC boundary conditions by means of image theory. This image theory is implemented by using ghost cell technique (Kim, 1997). If a wall is flat and lies along x-axis ($y = 0$), the values for the ghost cells (for more details, see Pranowo (2002)) are:

$$p(x, -y) = p(x, y) \quad (11)$$

D. Stability Criteria

The classic Courant criterion for stability of the Yee FDTD scheme is (Nguyen, 1996):

$$V_p \Delta t \sqrt{\left(\frac{1}{\Delta x}\right)^2 + \left(\frac{1}{\Delta y}\right)^2} \leq 1 \quad (12)$$

The left hand side of equation (12) is known as Courant or CFL number and V_p is the pressure wave velocity.

Dogaru (1999) proved that the MRTD equations are equivalent to the Yee FDTD equations obtained for a grid with step $\Delta x/2$ and $\Delta y/2$. Therefore, the stability criterion for MRTD with one level wavelet is (for more details, see Sarris et al. (2001)):

$$V_p \Delta t \sqrt{\left(\frac{2}{\Delta x}\right)^2 + \left(\frac{2}{\Delta y}\right)^2} \leq 1 \quad (13)$$

III. Numerical Results

A. One-dimensional case

To evaluate the accuracy of MRTD scheme, the following initial conditions are taken to perform numerical simulations:

$$\begin{aligned} u(x,0) &= 0 \\ p\left(x, \frac{\Delta t}{2}\right) &= \exp\left(\ln 2 x^2 / 9\right) \quad ; \quad -100 \leq x \leq 100 \end{aligned} \quad (14)$$

The results are compared to known exact solution, the exact solution in this case is:

$$p(x,t) = \left(\exp\left(\ln 2 \left((x-t)^2\right) / 9\right) + \exp\left(\ln 2 \left((x+t)^2\right) / 9\right) \right) / 2 \quad (15)$$

We take $\Delta t = 0.25$ and $\Delta x = 1$. Figure 5 shows the convergence rate of the root mean square error over the time interval $[0,50]$.

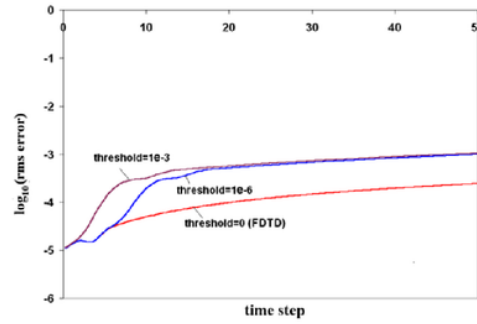


Fig. 5. Convergence rate for MRTD scheme

FDTD errors and MRTD errors are almost linear in time. As the absolute threshold increases, the numerical accuracy decreases. For long time running, accuracies of absolute threshold=1e-3 and 1e-6 get closer. Comparisons with the exact solution are shown in figure 6 for pressure (p) profile, a good agreements are found.

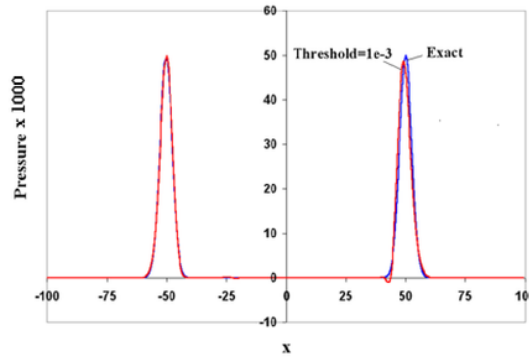


Fig. 6. Numerical solution of the 1-D acoustic problem at $t=50,125$

The number of coefficients for u and p after thresholding with absolute threshold=1e-6 and 1e-6 are compared to unthresholded coefficients (FDTD) for the same resolution.

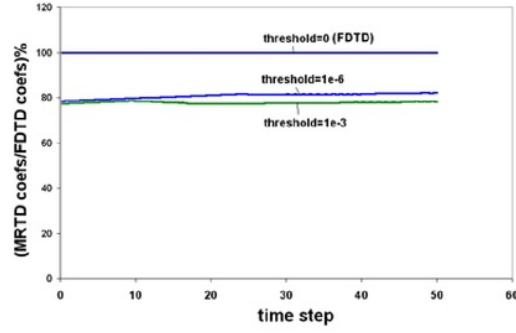


Fig. 7. Comparison of number coefficients in 1-d problem

A. Two-dimensional case

We next consider an acoustics wave propagation in a square cavity. We take the walls to be hard boundaries. The following initial conditions are applied:

$$\begin{aligned} u(x, y, 0) &= 0 \\ v(x, y, 0) &= 0 \\ p\left(x, y, \frac{\Delta t}{2}\right) &= \exp\left(-\ln 2 \frac{x^2 + (y-25)^2}{9}\right) \end{aligned} \quad ; \quad -100 \leq x \leq 100 \quad ; \quad 0 \leq y \leq 200 \quad (16)$$

We take $\Delta t = 0.25$, $\Delta x = 1$ and $\Delta y = 1$. Figure 8a – 8d show the propagation of the acoustic wave.

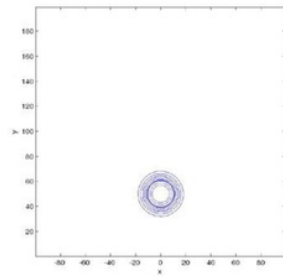


Fig. 8a. Pressure at t = 12.625

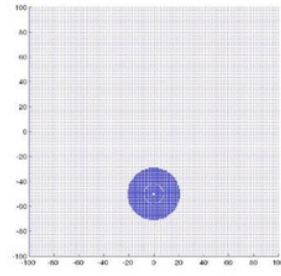


Fig. 9a. Mesh at t = 12.625, threshold=1e-3

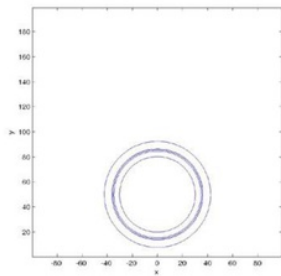


Fig. 8b. Pressure at t = 37.625

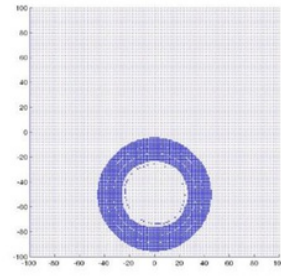


Fig. 9b. Mesh at t = 37.625, threshold=1e-3

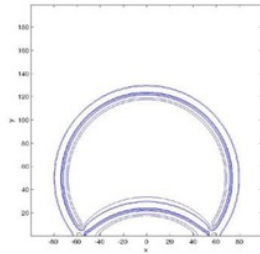


Fig. 8c. Pressure at $t = 75,125$

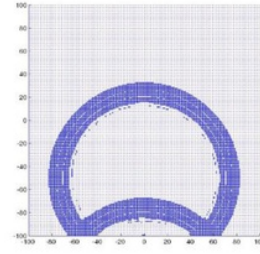


Fig. 9c. Mesh at $t = 75,125$, threshold= $1e-3$

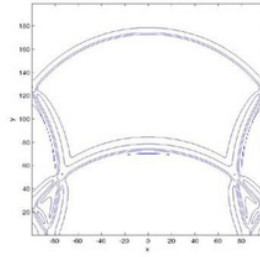


Fig. 8d. Pressure at $t = 125,125$

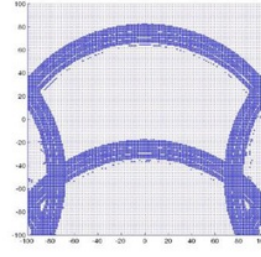


Fig. 9d. Mesh at $t = 125,125$, threshold= $1e-3$

It can be seen that a new source of wave propagation is created at the point of reflection, each time an incident wave is reflected by the wall. The points of reflection and the point where the waves met have higher gradient pressure. The mesh will be refined in regions of high pressure gradient via wavelet thresholding (figure 9a–9d).

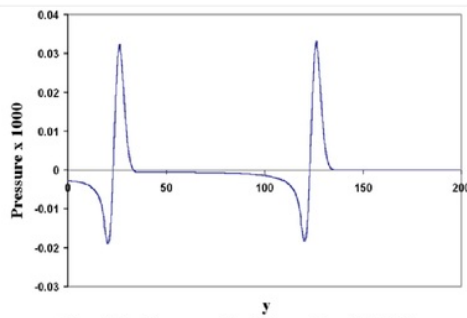


Fig. 10. Pressure Profile at $t = 75,125$

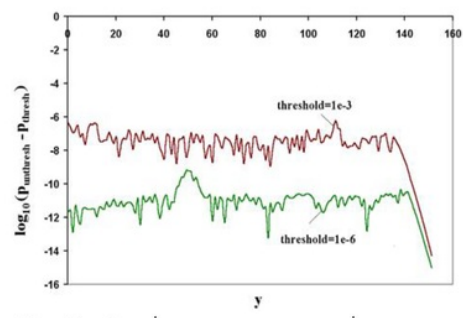


Fig. 11. $\log_{10}|p_{unthreshold} - p_{threshold}|$ at $t = 75,125$

Figure 10 & 11 show the pressure profile and absolute difference value of unthresholded and thresholded pressure at $x=0$. Computational effort can be reduced significantly using thresholding (figure 12).

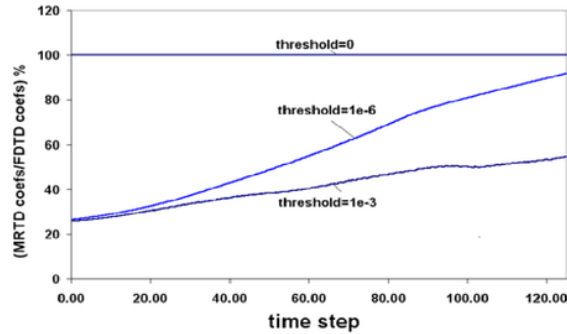


Fig. 12. Comparison of number coefficients in 2-d problem

IV. Conclusions

MRTD schemes based on Haar wavelet expansions are derived and applied in the numerical modeling of acoustic wave propagation. In this paper, it is shown that computational effort can be reduced without sacrificing solution accuracy. Implementation of the numerical is relatively simple and computed acoustic fields have a good agreement with exact solution.

For future research, we plan to extend the MRTD method for solving three-dimensional acoustic problems and use Daubechies wavelet family as the basis functions.

VI. Acknowledgement

The authors acknowledge illuminating discussions with Dr. Traian Dogaru of Department of Electrical Engineering, The Duke University via e-mail on the MRTD method based on Haar wavelet.

References

- Botteldoreen, D., 1995, *Finite-Difference Time-Domain Simulation of Low-Frequency Room Acoustic Problems*, Journal Acoustical Society of America, vol. 98, no. 6, pp. 3302-3308.
- Chiavassa, Guillaume, 1997, *Algorithmes Adaptatifs en Ondelletes pour la Resolution d'Equations aux Derivees Partielles*, These de Doctorat, Universite d'Aix-Marseille II.
- Daubechies, Ingrid, 1992, *Ten Lectures on Wavelets*, SIAM review, Philadelphia.
- Dogaru, Traian V., 1999, *Modelling and Signal Processing for Electromagnetic Subsurface Sensing*, Dissertation, The Duke University.
- Kim, Cheolwan, 1997, *Multidimensional Upwind Leapfrog Schemes and Their Applications*, PhD Thesis, The University of Michigan.
- Nguyen, Brian Tao, 1996, *Investigation of Three Level Finite Difference Time Domain Methods for Multidimensional Acoustics and Electromagnetics*, PhD Thesis, The University of Michigan.
- Sarris, Costas D., Katehi, Linda P. B. and Harvey, James F., 2000, *Application of Multiresolution Analysis to Modeling of Microwave and Optical Structures* Journal of Optical and Quantum Electronics, Kluwer Academic Publisher.
- Sarris, Costas D. and Katehi, Linda P. B., 2001, *Some Aspect of Dispersion Analysis of Multiresolution Time Domain Schemes*, Proceedings of the 17th Annual Review of Progress in Applied Computational Electromagnetics, pp: 23-30.
- Schneider, J. B. and Ramahi, O. M., 1998, *The Complementary Operators Method Applied to Acoustic Finite-Difference Time-Domain Simulations*, Journal of the Acoustical Society of America, vol. 104, no. 2, pt. 1, pp. 686-693.

- Tentzeris, Emmanouil M., Robertson R. L., Katehi L. P. B., 1997, *Space and Time Adaptive Gridding Using MRTD Technique*, MTTS-S Digest, pp. 337-339.
- Pranowo, 2002, Metode Multiresolusi di Kawasan Waktu untuk Penyelesaian Numerik Persamaan Maxwell dan Akustik, Master Thesis, The Gadjah Mada University.

ORIGINALITY REPORT

21%

SIMILARITY INDEX

15%

INTERNET SOURCES

21%

PUBLICATIONS

6%

STUDENT PAPERS

PRIMARY SOURCES

<div style="background-color: red; color: white; width: 40px; height: 40px; display: flex; align-items: center; justify-content: center; margin-bottom: 10px;">1</div>	<p>Kavita Goverdhanam, Costas D. Sarris, Manos M. Tentzeris, Linda P. B. Katehi. "A Perfectly Matched Layer Absorber Formulation for Haar Wavelet Based MRTD", 29th European Microwave Conference, 1999, 1999</p> <p>Publication</p>	<div style="font-size: 2em; font-weight: bold;">4%</div>
--	--	--

<div style="background-color: magenta; color: white; width: 40px; height: 40px; display: flex; align-items: center; justify-content: center; margin-bottom: 10px;">2</div>	<p>Guy V. Norton, Robert D. Purrington. "The Westervelt equation with viscous attenuation versus a causal propagation operator: A numerical comparison", Journal of Sound and Vibration, 2009</p> <p>Publication</p>	<div style="font-size: 2em; font-weight: bold;">3%</div>
--	--	--

<div style="background-color: purple; color: white; width: 40px; height: 40px; display: flex; align-items: center; justify-content: center; margin-bottom: 10px;">3</div>	<p>www.dafx12.york.ac.uk</p> <p>Internet Source</p>	<div style="font-size: 2em; font-weight: bold;">2%</div>
---	--	--

<div style="background-color: teal; color: white; width: 40px; height: 40px; display: flex; align-items: center; justify-content: center; margin-bottom: 10px;">4</div>	<p>people.ee.duke.edu</p> <p>Internet Source</p>	<div style="font-size: 2em; font-weight: bold;">2%</div>
---	--	--

<div style="background-color: green; color: white; width: 40px; height: 40px; display: flex; align-items: center; justify-content: center; margin-bottom: 10px;">5</div>	<p>T. Dogaru, L. Carin. "Application of Haar-wavelet-based multiresolution time-domain schemes to electromagnetic scattering problems", IEEE Transactions on Antennas and</p>	<div style="font-size: 2em; font-weight: bold;">2%</div>
--	---	--

Propagation, 2002

Publication

6	asa.scitation.org Internet Source	1%
7	QUNSHENG CAO, YINCHAO CHEN. "MRTD analysis of a transient electromagnetic pulse propagating through a dielectric layer", International Journal of Electronics, 2010 Publication	1%
8	Y. Liu, I.T. Cameron, F.Y. Wang. "The wavelet-collocation method for transient problems with steep gradients", Chemical Engineering Science, 2000 Publication	1%
9	e-journal.uajy.ac.id Internet Source	1%
10	Submitted to Universitas Atma Jaya Yogyakarta Student Paper	1%
11	www.brianhamilton.co Internet Source	1%
12	M.M. Cerimele, F. Pistella, R.M. Spitaleri. "Numerical simulations of acoustic fields on boundary-fitted grids", Mathematics and Computers in Simulation, 2008 Publication	1%

Submitted to North West University

13

Student Paper

1%

14

www.dcabes2018.com

Internet Source

1%

Exclude quotes On

Exclude matches < 1%

Exclude bibliography On

FINAL GRADE

/0

GENERAL COMMENTS

Instructor

PAGE 1

PAGE 2

PAGE 3

PAGE 4

PAGE 5

PAGE 6

PAGE 7

PAGE 8

PAGE 9